Available online at www.sciencedirect.com
ScienceDirect
Combustion and Flame 152 (2008) 60–68
Combustion and Flame
www.elsevier.com/locate/combustflame

Lengths of laminar jet diffusion flames under elevated gravity

Peter B. Sunderland [a,*], James E. Haylett [b], David L. Urban [c], Vedha Nayagam [b]

[a] *Department of Fire Protection Engineering, University of Maryland, College Park, MD 20742, USA*
[b] *National Center for Space Exploration Research, Cleveland, OH 44135, USA*
[c] *NASA Glenn Research Center, Cleveland, OH 44135, USA*

Received 3 January 2007; received in revised form 1 August 2007; accepted 31 August 2007

Abstract

There are two prevalent scaling relationships for lengths of laminar jet diffusion flames on circular burners. Experimental studies of earth-gravity and microgravity flames generally invoke a linear relationship between normalized flame length and Reynolds number. In contrast, most studies conducted at elevated gravity have correlated flame lengths with a function of Reynolds and Froude numbers. An important distinction between these scalings is that the Reynolds scaling indicates that stoichiometric flame length is independent of gravity level, whereas the Reynolds–Froude scaling indicates that length decreases with increased gravity. The present work examines the ability of both approaches to correlate laminar hydrogen, methane, ethane, and propane flame lengths for a range of 1–15 times earth gravity. The Reynolds scaling is shown to accurately correlate the length measurements at both earth gravity and elevated gravity. The Reynolds–Froude scaling also correlates the measurements, but its theoretical basis is less rigorous, it does not account as accurately for variations in fuel flowrate, it does not admit microgravity flames, and past predictions of its behavior at low and high Froude number are not supported even with the present extension of Froude number to over eight orders of magnitude. It is shown that the observed reduction in *luminosity* length at elevated gravity can be attributed to soot interference and that *stoichiometric* flame length is independent of gravity except in the approach to microgravity.
Published by Elsevier Inc. on behalf of The Combustion Institute.

Keywords: Centrifuge; Flame shape; Microgravity; Slot burner; Soot

1. Introduction

Flame shape, and in particular flame length, is a fundamental property of laminar jet diffusion flames that is readily measured and modeled. Since the seminal work of Burke and Schumann [1], dozens of studies have measured the lengths of such flames. Most were conducted under earth gravity, although considerable attention has been paid to microgravity conditions, as discussed in Refs. [2–8] and references therein. An understanding of laminar flame shapes and their scaling is important in the planning and analysis of combustion research, both experimental and computational, and in the design of industrial burners.

* Corresponding author. Fax: +1 301 405 9383.
E-mail address: pbs@umd.edu (P.B. Sunderland).

0010-2180/$ – see front matter Published by Elsevier Inc. on behalf of The Combustion Institute.
doi:10.1016/j.combustflame.2007.08.011

Just three research groups have measured laminar gas jet diffusion flame lengths at elevated gravity: Altenkirch and co-workers [9–11], Durox et al. [12], and Arai and co-workers [13–16]. Past work at elevated gravity has correlated flame lengths with a different scaling than is normally used in earth-gravity and microgravity work. This is significant because one choice predicts flame length to be independent of gravity level whereas the other indicates a decrease of flame length with increased gravity. The present study is an examination of this issue.

As discussed by Sunderland et al. [5], many theoretical and numerical models [17–23] have arrived independently at a Reynolds scaling of

$$L/d \sim \mathrm{Re} \tag{1}$$

for a given fuel and oxidizer burning on circular burners, where L is laminar flame length, d is burner diameter, $\sim$ represents proportionality, and Re is the Reynolds number, defined below. Length L is defined by most models to be the stoichiometric flame length, but many experimental studies instead take L to be the luminous flame length. Equation (1) is widely accepted for nonbuoyant flames. Several models, e.g., Roper [18], also predict this behavior at buoyant conditions [5]. For a given fuel and oxidizer, Eq. (1) indicates that flame length is proportional to fuel mass flowrate and is independent of pressure, burner diameter, and gravity level. This predicted independence from gravity is of particular interest here. This scaling has been validated by numerous experiments under microgravity and earth gravity [1–6,17–24]. Studies of elevated-gravity flames have considered this scaling [10,11,16], but have favored the Reynolds–Froude scaling of Altenkirch et al. [9].

The development of Altenkirch et al. [9] began with a balance between fuel and oxidizer supply rates following Jost [17]. It is noteworthy that this balance reduces to Eq. (1) when the diffusion length scales with the flame width. Rather than matching these lengths, Ref. [9] approximated the diffusion length as the thickness of a natural-convection boundary layer on an isothermal vertical flat plate,

$$\delta/x \sim \left(gx^3/\nu^2\right)^{-1/4}, \tag{2}$$

where δ is the momentum boundary-layer thickness, x is the streamwise distance from the leading edge, g is the local acceleration of gravity, and ν is the kinematic viscosity. The application of this flat-plate solution to axisymmetric flames is not well supported because the transverse curvature of the boundary layer generally is significant in these flames, but for a given fuel and oxidizer it led to

$$L/d \sim \mathrm{Re}^{2/3}\,\mathrm{Fr}^{1/3}(w/d)^{-4/3}, \tag{3}$$

where the Reynolds and Froude numbers are defined as

$$\mathrm{Re} = ud/\nu; \qquad \mathrm{Fr} = u^2/(gd). \tag{4}$$

Here w is the maximum flame width and u is the fuel source average velocity. Altenkirch et al. [9] suggested that w/d is nearly constant for a given choice of fuel and oxidizer, and, using their experimental data, noted two limiting tends, for large and small Fr:

$$L/d \sim \mathrm{Re}^{2/3}, \quad \text{nonbuoyant limit (large Fr)}, \tag{5a}$$

$$L/d \sim \mathrm{Re}^{2/3}\,\mathrm{Fr}^{1/3}, \quad \text{buoyant limit (small Fr)}. \tag{5b}$$

The application of a buoyant boundary-layer solution, Eq. (2), in the derivation of the nonbuoyant scaling of Eq. (5a) is not well-founded; a preferable method for nonbuoyant flames would be to use the classical solution for boundary-layer thickness associated with forced convection over a flat plate:

$$\delta/x \sim (ux/\nu)^{-1/2}. \tag{6}$$

Although this is preferable for nonbuoyant flames, it nevertheless involves applying a flat-plate solution to an axisymmetric configuration. This diffusion length leads to the Reynolds scaling of Eq. (1) rather than the relationships of Eqs. (3) and (5a). It is noteworthy how many ways there are to arrive at this scaling.

There are three significant shortcomings in the Reynolds–Froude scaling of Eqs. (5):

1. The flat-plate boundary-layer solution is invoked but it is invalid for most axisymmetric flames. Sparrow and Gregg [25] found transverse curvature to be important for buoyant flows over vertical isothermal cylinders when $D/L \leqslant 35/\mathrm{Gr}^{1/4}$, where D and L are the cylinder diameter and length and Gr is the Grashof number.
2. Equation (5a) is a solution for nonbuoyant flames that is predicated on a buoyant flat-plate solution.
3. Constant w/d is invoked. Although this behavior has been observed in microgravity flames at large Re [5,6], it has not been reported either in microgravity flames at lower Re or in normal-gravity flames [5]. It should be noted that microgravity flame observations were very limited when these relationships were developed.

Despite these shortcomings, Altenkirch et al. [9] applied the Reynolds–Froude scaling of Eqs. (5) in correlating their flame length measurements. This approach was later adopted by Rosner [26], Durox and co-workers [12,22], and Sato et al. [16] in correlating the lengths of elevated-gravity flames. The choice of plot axes suggested by Eqs. (5) yields reasonable correlations. These correlations imply a decrease of flame length with increasing gravity. Such a decrease agrees with observations of luminosity lengths of laminar hydrocarbon flames, but whether it applies also to stoichiometric lengths requires further examination. Empirical support has been weak for both the low-Fr or high-Fr predictions of Eqs. (5).

Thus motivated, the objectives of the present work are to examine the relative merits of these two scaling laws with respect to flame length measurements in centrifuge facilities and to evaluate whether soot interference could be responsible for the observed reduction in luminosity length at elevated gravity. Existing measurements are supplemented with new numerical predictions of flame lengths to examine soot interference and to extend the range of conditions.

Lengths of turbulent condensed-fuel fires and pool-fire-type flames have been predicted [27] and observed in a centrifuge [28] to scale with $g^{-1/3}$. These interesting findings are beyond the scope of this work because they involve turbulent phenomena.

2. Length scaling for slot-burner flames

Further insight into the above scalings for axisymmetric flames is available by considering solutions for slot-burner flames. Roper [18] solved conservation of mass and species to find the concentration fields of flames on circular, square, and slot burners. His analysis predicted that stoichiometric lengths of flames on circular and square burners scale according to Eq. (1) and thus are independent of gravity level. In contrast, he found that flames burning on long slot burners behave according to

$$L/b \sim \mathrm{Re}, \quad \text{nonbuoyant limit (large Fr)}, \qquad (7a)$$

$$L/b \sim \mathrm{Re}^{2/3}\,\mathrm{Fr}^{1/3}, \quad \text{buoyant limit (small Fr)}, \qquad (7b)$$

where b is the slot width, which here is the length scale for both Re and Fr.

The Altenkirch et al. [9] development can be modified for flames burning on long slot burners as follows. When the diffusion lengths are taken to be the planar boundary layer thicknesses of Eqs. (2) and (6) for buoyant and nonbuoyant flames, respectively, this yields the Roper scalings of Eqs. (7). These planar boundary layer approximations are more justifiable for slot-burner flames than for most axisymmetric flames. This development does not suffer from any of the three shortcomings listed above that are associated with Eqs. (5) for axisymmetric flames.

For slot-burner flames, the Altenkirch et al. [9] method avoids these shortcomings and agrees with Roper [18]. For axisymmetric flames Altenkirch et al. [9] cannot avoid the shortcomings and it departs from Roper. These observations indicate that the theoretical basis of the Reynolds scaling, Eq. (1), is stronger than that of Eqs. (5) for flame lengths at elevated gravity.

3. Computations

Past measurements of flame lengths at elevated gravity generally considered luminous lengths. In contrast, stoichiometric lengths are more relevant to the scaling predictions of Eqs. (1) and (5). To examine this difference, and to extend the range of conditions considered, a computational fluid dynamics (CFD) model was developed for methane flames. The model furnishes predictions of stoichiometric flame lengths, which can be used to test the two scaling relationships.

The CFD model solves conservation equations for mass, momentum, energy, and species using the COMPACT-2D code, which implements the SIMPLE algorithm developed by Patankar [29]. Both radial and axial diffusion are included. The model assumes steady laminar axisymmetric flow, infinitely fast single-step chemistry, the absence of soot, and negligible radiation. Gas properties (viscosity, thermal conductivity, mass diffusivity, and specific heat) are taken to be constant everywhere, but temperature and density are allowed to vary. The model allows gravity level to be specified. More advanced CFD models are available, e.g., Linteris et al. [30] and Smooke et al. [31], but the present simplifications are not expected to have an impact on the findings.

The computational domain has 80 axial and 40 radial grids. A weak coflow condition (ca. 1% of the fuel velocity) is specified at the upstream boundary, symmetry is specified on the axis, and a constant-pressure condition is specified at the other boundaries. Relative to the burner, the domain extends approximately two flame lengths downstream, one flame length upstream, and two flame widths radially. Grid independence was verified by modifying the domain size and the number of grids and observing no significant change in predicted flame shape. The model predictions are in reasonable agreement with the observed stoichiometric shapes of normal-gravity methane flames observed by the authors.

4. Results and discussion

Many studies have measured the lengths of laminar gas jet diffusion flames. Several of these [2–5, 9–12,14–16,23,32,33] contain measurements that are included here, as summarized in Table 1. Nomenclature in this table includes $G = g/g_e$, where $g_e = 9.81\ \mathrm{m/s^2}$, and p, ambient pressure. This table, and the plots that follow, include all known measurements

Table 1
Sources of flame observations and model and the associated conditions considered in the present work, all involving laminar flames of pure fuel burning in air on circular burners

Source	Fuel	Air	G	d (mm)	p (bar)
Altenkirch and co-workers[a]	H_2, CH_4, C_2H_6, C_3H_8	Coflowing	1–15	0.8–2.1	1
Arai and co-workers[b]	CH_4, C_3H_8	Quiescent	1–9	2–7.5	1
Cochran and co-workers[c]	H_2, CH_4	Quiescent	1	1.02–8.84	0.98
Durox et al. [12]	CH_4	Coflowing	1–8.5	2.2, 12	1
Li et al. [23]	CH_4	Coflowing	1	16	1
Saito and co-workers[d]	CH_4, C_2H_6	Quiescent	1	0.41	1
Sunderland et al. [5]	CH_4, C_2H_6, C_3H_8	Quiescent	1	0.19–5.5	0.25–1.97
Present model	CH_4	Quiescent	1–8	0.19–12	1

[a] Altenkirch et al. [9], Brancic [10], and Cevallos [11].
[b] Arai et al. [14,15] and Sato et al. [16].
[c] Cochran and Masica [2], Cochran [3], and Haggard and Cochran [4].
[d] Ban et al. [32] and Nakamura et al. [33].

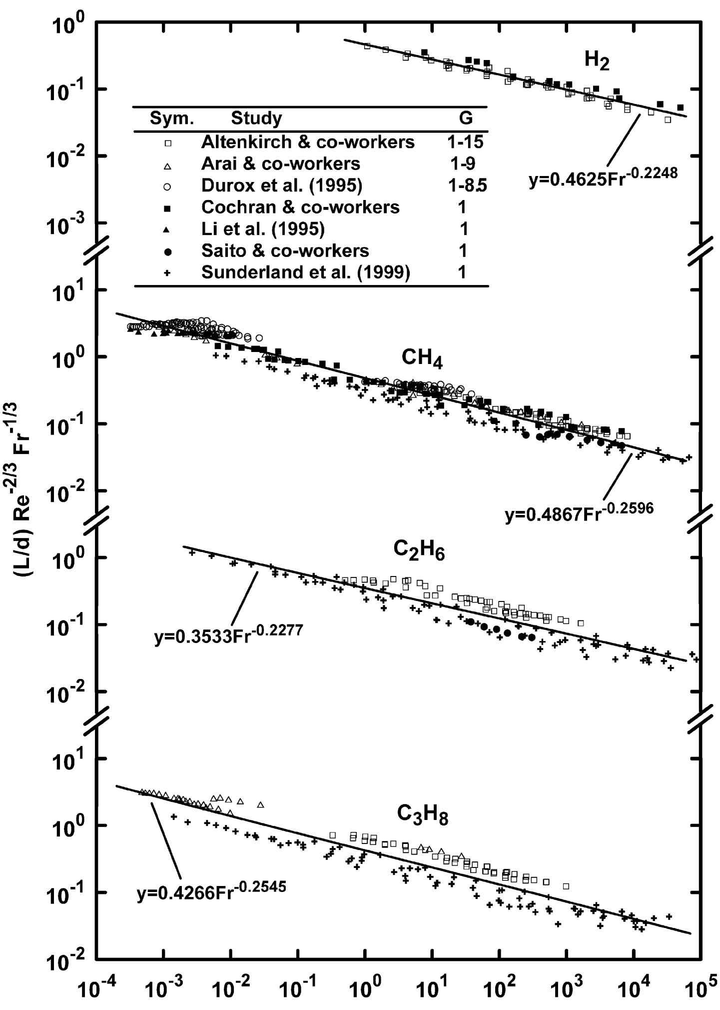

Fig. 1. Laminar flame length relationship of Altenkirch et al. [9] for H_2, CH_4, C_2H_6, and C_3H_8 fueled flames on circular burners at various gravity levels. Citations for the legend entries are given in Table 1. The lines and equations shown are best fits, where y is defined as $(L/d)\,\mathrm{Re}^{-2/3}\,\mathrm{Fr}^{-1/3}$.

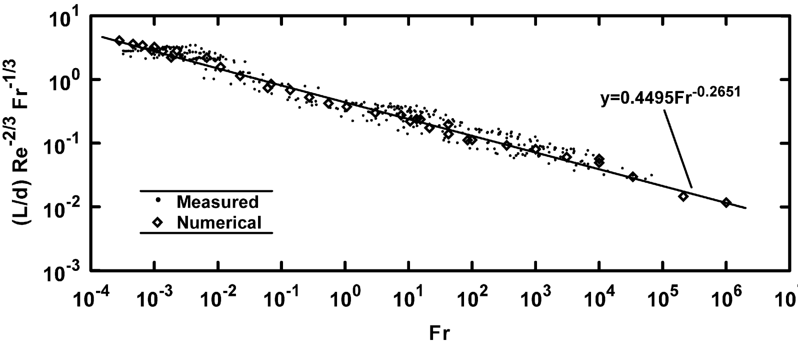

Fig. 2. Laminar flame length relationship of Altenkirch et al. [9] for CH_4-fueled flames for the measurements of Fig. 1 and the present numerical results. The line and equation is a best fit of the numerical data only, where y is defined as $(L/d)\,\mathrm{Re}^{-2/3}\,\mathrm{Fr}^{-1/3}$.

of steady laminar flame lengths at elevated gravity for the four fuels considered. Indication of coflowing or quiescent air is included in Table 1. However, the experimental results do not reveal any effect of coflow on flame length; see Roper et al. [19] and Lin and Faeth [24]. Also shown in Table 1 is the range of conditions considered using the present numerical model.

To test their scaling given in Eq. (3), Altenkirch et al. [9] plotted their measurements using Fr and $(L/d)\,\mathrm{Re}^{-2/3}\,\mathrm{Fr}^{-1/3}$ as axes, an approach that was followed by others [12,16,22,26] and that is shown in Fig. 1 for the studies of Table 1. (Herein dynamic viscosity is assigned published values of 8.76, 10.9, 9.22, and 8.05 $\mathrm{mg/(m\,s)}$ for H_2, CH_4, C_2H_6, and C_3H_8, respectively.) The data correlation in Fig. 1 is reasonable. However, in addition to its theoretical weaknesses mentioned above, this choice of axes has several drawbacks: L/d does not appear alone, Fr is included in both the abscissa and the ordinate, and microgravity flames are not admitted. The fits of Fig. 1 suggest a decrease of flame length with increasing gravity with an approximate scaling of $L \sim g^{-0.1}$.

Several experimental studies have claimed two intriguing trends in such plots: that the data are correlated by a slope of 0 at low Fr [9,22,26] and a slope of $-1/3$ at high Fr [9,26]. Such behavior is predicted by Eqs. (5b) and (5a), respectively. The present inclusion of additional measurements extends the range of Fr four orders lower and one order higher here than in the initial work [9]. Nevertheless, empirical support is absent for either of these predictions.

Fig. 2 shows the methane flame data from Fig. 1 using the same axes with the addition of the present numerical predictions for several flames. The correlation of the numerical predictions is similar to that of the measurements. The numerical data extend to higher Fr than do the experiments and still do not exhibit the type of high-Fr behavior of Eq. (5a) that was suggested by Refs. [9,26].

The measurements and computations in Figs. 1 and 2 generally fall above the linear fits for high fuel mass flow rates and below the fits for low mass flow rates. Such behavior does not occur when L/d is plotted versus Re, below. Length correlations such as those in Figs. 1 and 2 do not properly account for variations in fuel mass flowrate, which contributes to the data scatter in these plots.

Motivated by many past publications, L/d is plotted versus Re in Fig. 3 for the same measurements as shown in Fig. 1. The data are well correlated and do not exhibit the mass flowrate discrepancy of the Altenkirch et al. [9] correlation. The data exhibit a slope slightly larger than the unity slope of the theory, indicating that Eq. (1) does not capture all the physics involved. One factor here is that the theory does not account for flames at low Re, which can attach below the burner tip, and flames at high Re, which can be slightly lifted. Introduction of a virtual origin [6,24] could reduce the slope of the data in Fig. 3. Microgravity flames also have been included on the axes of Fig. 3 [2–6,24], revealing increased lengths that have been attributed to various mechanisms [5,6]. Fig. 3 lends support to the scaling $L/d \sim \mathrm{Re}$ regardless of gravity level.

Fig. 4 shows the methane flame data from Fig. 3 using the same axes with the addition of the present numerical predictions for several flames. The correlation of the numerical predictions again is similar to that of the measurements. The numerical data extend to higher Re than do the experiments. Like the measurements, the computed lengths exhibit a slope slightly larger than unity.

Despite the success of Figs. 3 and 4 in correlating flame lengths in earth gravity and elevated gravity, all the present centrifuge studies reported decreased luminosity lengths at elevated gravity. This could arise

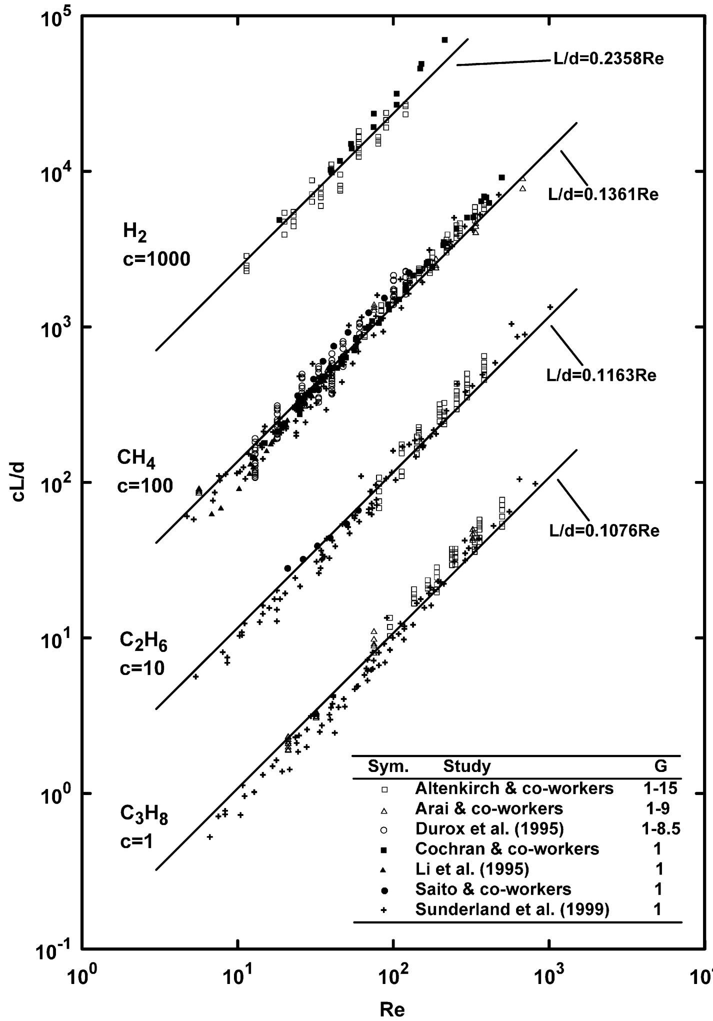

Fig. 3. Normalized flame length as a function of Reynolds number for H_2, CH_4, C_2H_6, and C_3H_8 flames on circular burners at various gravity levels. Citations for the legend entries are given in Table 1. The data are the same as those plotted in Fig. 1. The lines and equations shown are best fits predicated on unity slope. The L/d values for all fuels except propane are shifted upward by a factor c, as shown, to avoid plot overlap.

from soot interference, whereas stoichiometric flame length could be unaffected by gravity except in the approach to microgravity. Luminosity lengths of earth-gravity hydrocarbon-fueled flames typically exceed stoichiometric lengths by 10–60% [6,20,24,34] in a way that has been correlated [21,24]. Increased gravity decreases the residence time available for soot formation and can change hydrocarbon flames from yellow to blue [9,13–16], but it may have little or no effect on stoichiometric flame length.

To address this issue, Fig. 5 is a plot of flame length normalized as $L/(d\,\mathrm{Re})$ versus G for the same measurements considered earlier. Owing to the empirical support for Eq. (1) apparent in Fig. 3, any statistical variation in $L/(d\,\mathrm{Re})$ with gravity should quantify the dependence of flame length on gravity level. The hydrogen flame lengths in Fig. 5 (which are stoichiometric lengths) reveal the smallest decrease in flame length at elevated gravity. Much of this decrease for hydrogen may arise from curved flames associated with Coriolis effects, estimated by Ref. [9] to bias the measured flame lengths downward by up to 6% at elevated gravity. Note that the dimness of hydrogen flames [4,10], particularly at their tips, complicates their length measurements.

In Fig. 5 the hydrocarbon flames reveal substantially reduced lengths at elevated gravity. This is attributed here to soot interference because these lengths are luminosity lengths. At the highest gravity levels, where soot interference is minimized, the

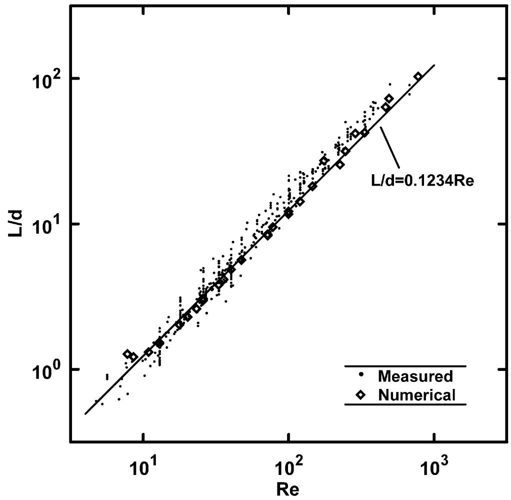

Fig. 4. Normalized flame length as a function of Reynolds number for CH_4-fueled flames for the measurements of Fig. 3 and the present numerical results. The line and equation are a best fit of the numerical data only.

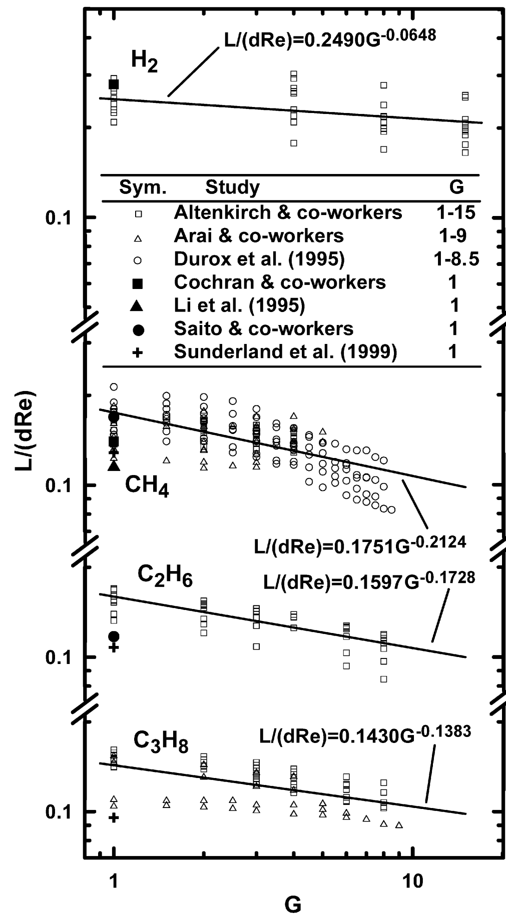

Fig. 5. Effect of gravity level on $L/(d\,\mathrm{Re})$ for H_2, CH_4, C_2H_6, and C_3H_8 flames on circular burners. Citations for the legend entries are given in Table 1. The open symbols correspond to individual measurements. The other symbols correspond to geometric means of earth-gravity measurements. The lines and equations shown are best fits of the open symbols.

luminosity lengths of the hydrocarbon flames match the plotted geometric means of the earth-gravity stoichiometric lengths, reported by Ref. [5] at otherwise comparable conditions.

Fig. 6 shows the methane flame data from Fig. 5 using the same axes, with the addition of the present numerical predictions. Here the computed methane flames reveal only a small decrease in normalized stoichiometric flame length at elevated gravity. In contrast, the measured luminosity lengths decrease more rapidly when gravity is increased. The computations of Fig. 6 support the key observation of Fig. 5, namely that stoichiometric flame length is practically independent of gravity level.

None of the correlations of Figs. 1–4 is perfect; neither the Reynolds scaling nor the Reynolds–Froude scaling accounts fully for the complexity of these flames. These simple models neglect soot interference, axial diffusion, radiation, unsteadiness, burner heat loss, flame attachment below or above the burner tip, reactant leakage, and Coriolis effects. While the overall scatter in these length correlations is similar under both scalings, it is statistically significant that the Reynolds scaling accounts better for fuel flowrate variations.

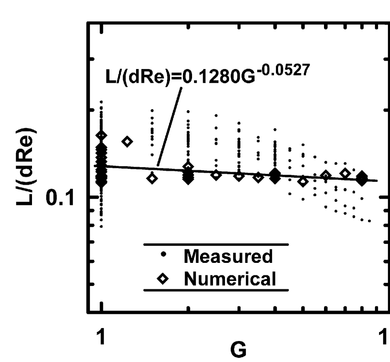

Fig. 6. Effect of gravity level on $L/(d\,\mathrm{Re})$ for CH_4 flames for the measurements of Fig. 5 and the present numerical results. The line and equation are a best fit of the numerical data only.

5. Conclusions

Two scaling laws of laminar gas jet diffusion flame lengths at elevated gravity were examined. The length predictions of Roper [18] and Altenkirch et al. [9] differ for flames on circular burners, but for slot-burner flames an extension here of the Altenkirch et al. [9] method agrees with the Roper prediction. Correlations for circular burners using both predictions were presented for H_2, CH_4, C_2H_6 and C_3H_8 flame lengths from both earth-gravity and elevated-gravity facilities. The major conclusions for flames on circular burners are as follows:

1. Stoichiometric flame lengths at normal and elevated gravity are independent of gravity level within experimental uncertainties. The decrease in hydrocarbon flame luminosity length with increased gravity can be attributed to soot interference.
2. Measured and computed flame lengths are well correlated according to the Reynolds scaling of $L/d \sim \text{Re}$. This scaling has strong theoretical and empirical support for microgravity, normal gravity, and elevated gravity flames.
3. The Reynolds–Froude length scaling of Altenkirch et al. [9] has several disadvantages relative to the Reynolds scaling. It does not account as well for variations in fuel mass flowrate and its associated plot axes have less utility. It neglects transverse curvature effects and thus is more appropriate for flames on slot burners.
4. Past predictions for the behavior of the Altenkirch et al. [9] scaling at low and high Fr are not supported by measurements or computations.

Existing measurements from centrifuge facilities have been limited to a pressure of 1 bar and most have not minimized soot interference or reported flame widths. Future observations of elevated-gravity flames could address these limitations.

Acknowledgments

This work was supported by NASA Office of Biological and Physical Sciences Grant NNC-05GA59G, under the management of Merrill K. King. We appreciate helpful discussions with John L. de Ris and Gregory T. Linteris.

References

[1] S.P. Burke, T.E.W. Schumann, Ind. Eng. Chem. 20 (10) (1928) 998–1004.
[2] T.H. Cochran, W.J. Masica, Proc. Combust. Inst. 13 (1970) 821–829.
[3] T.H. Cochran, Experimental Investigation of Laminar Gas Jet Diffusion Flames in Zero Gravity, NASA TN D-6523, 1972.
[4] J.B. Haggard Jr., T.H. Cochran, Hydrogen and Hydrocarbon Diffusion Flames in a Weightless Environment, NASA TN D-7165, 1973.
[5] P.B. Sunderland, B.J. Mendelson, Z.-G. Yuan, D.L. Urban, Combust. Flame 116 (1999) 376–386.
[6] K.-C. Lin, G.M. Faeth, P.B. Sunderland, D.L. Urban, Z.-G. Yuan, Combust. Flame 116 (1999) 415–431.
[7] P.B. Sunderland, S.S. Krishnan, J.P. Gore, Combust. Flame 136 (2004) 254–256.
[8] C. Aalburg, F.J. Diez, G.M. Faeth, P.B. Sunderland, D.L. Urban, Z.-G. Yuan, Combust. Flame 142 (2005) 1–16.
[9] R.A. Altenkirch, R. Eichhorn, N.N. Hsu, A.B. Brancic, N.E. Cevallos, Proc. Combust. Inst. 16 (1976) 1165–1174.
[10] A.B. Brancic, Effect of Increased Gravity on Laminar Diffusion Flames, M.S. thesis, University of Kentucky, Lexington, 1976.
[11] N.E. Cevallos, Experimental Studies of Effects of Elevated Gravity on Gaseous Hydrocarbon Diffusion Flames, M.S. thesis, University of Kentucky, Lexington, 1976.
[12] D. Durox, T. Yuan, F. Baillot, J.M. Most, Combust. Flame 102 (1995) 501–511.
[13] K. Amagai, Y. Ito, M. Arai, J. Jpn. Soc. Micrograv. Appl. 14 (1) (1997) 3–9.
[14] M. Arai, K. Amagai, Y. Ito, in: Proc. Second Int. Symp. Scale Modeling, Lexington, KY, 1997, pp. 197–210.
[15] M. Arai, H. Sato, K. Amagai, Combust. Flame 118 (1999) 293–300.
[16] H. Sato, K. Amagai, M. Arai, Combust. Flame 123 (2000) 107–118.
[17] W. Jost, Explosion and Combustion Processes in Gases, McGraw–Hill, New York, 1946, p. 212.
[18] F.G. Roper, Combust. Flame 29 (1977) 219–226.
[19] F.G. Roper, C. Smith, A.C. Cunningham, Combust. Flame 29 (1977) 227–234.
[20] R.E. Mitchell, A.F. Sarofim, L.A. Clomburg, Combust. Flame 37 (1980) 227–244.
[21] K. Saito, F.A. Williams, A.S. Gordon, Combust. Sci. Technol. 21 (1986) 117–138.
[22] E. Villermaux, D. Durox, Combust. Sci. Technol. 84 (1992) 279–294.
[23] S.C. Li, A.S. Gordon, F.A. Williams, Combust. Sci. Technol. 104 (1995) 75–91.
[24] K.-C. Lin, G.M. Faeth, AIAA J. 37 (6) (1999) 759–765.
[25] E.M. Sparrow, J.L. Gregg, J. Heat Transfer 78 (1956) 1823–1829.
[26] D.E. Rosner, Transport Processes in Chemically Reacting Flow Systems, Dover, Mineola, NY, 2000, p. 435.
[27] J.G. Quintiere, Fire Safety J. 15 (1989) 3–29.
[28] J.-M. Most, P. Mandin, J. Chen, P. Joulain, D. Durox, A.C. Fernandez-Pello, Proc. Combust. Inst. 26 (1996) 1311–1317.
[29] S.V. Patankar, Numerical Heat Transfer and Fluid Flow, Hemisphere, New York, 1980.
[30] G.T. Linteris, F. Takahashi, V.R. Katta, Combust. Flame 149 (2007) 91–103.

[31] M.D. Smooke, M.B. Long, B.C. Connelly, M.B. Colket, R.J. Hall, Combust. Flame 143 (2005) 613–628.
[32] H. Ban, S. Venkatesh, K. Saito, J. Heat Transfer 116 (1994) 954–959.
[33] Y. Nakamura, H. Ban, K. Saito, T. Takeno, in: Proc. Spring Tech. Meeting Central States Section, The Combustion Institute, Pittsburgh, 1997, pp. 160–163.
[34] A. Gomez, G. Sidebotham, I. Glassman, Combust. Flame 58 (1984) 45–57.